

# Observation of persistent orientation of chiral molecules by laser field with twisted polarization

Ilya Tutunnikov,<sup>1</sup> Johannes Floß,<sup>2</sup> Erez Gershnel,<sup>1</sup> Paul Brumer,<sup>2</sup> Ilya Sh. Averbukh,<sup>1, a)</sup> Alexander A. Milner,<sup>3</sup> and Valery Milner<sup>3, b)</sup>

<sup>1)</sup> AMOS and Department of Chemical and Biological Physics, The Weizmann Institute of Science, Rehovot 7610001, Israel

<sup>2)</sup> Chemical Physics Theory Group, Department of Chemistry, and Center for Quantum Information and Quantum Control, University of Toronto, Toronto, ON M5S 3H6, Canada

<sup>3)</sup> Department of Physics & Astronomy, The University of British Columbia, Vancouver, BC V6T 1Z1, Canada

Molecular chirality is an omnipresent phenomenon of fundamental significance in physics, chemistry and biology. For this reason, search for novel techniques for enantioselective control, detection and separation of chiral molecules is of particular importance. It has been recently predicted that laser fields with twisted polarization may induce persistent enantioselective field-free orientation of chiral molecules. Here we report the first experimental observation of this phenomenon using propylene oxide molecules ( $\text{CH}_3\text{CHCH}_2\text{O}$ , or PPO) spun by an optical centrifuge - a laser pulse, whose linear polarization undergoes an accelerated rotation around its propagation direction. We show that PPO molecules remain oriented on a time scale exceeding the duration of the centrifuge pulse by several orders of magnitude. The demonstrated long-time field-free enantioselective orientation opens new avenues for optical manipulation, discrimination, and, potentially, separation of molecular enantiomers.

Chiral molecules exist in two nonsuperimposable forms called enantiomers (1). The ability to analyze and separate mixtures of enantiomers is crucial, for example, in drug synthesis as different enantiomers of chiral molecules may exhibit strikingly different biological activity. Over the years, various optical approaches have been developed to control molecules in the gas phase and induce their alignment/orientation (for recent reviews, see e.g. (2–5)). The most known technique of this kind is field-free *alignment* of linear molecules by short linearly polarized laser pulses, which makes the most polarizable molecular axis point along the polarization direction after the end of the pulse (6). Laser-induced molecular *orientation* is a more challenging task; however, several techniques have been suggested and demonstrated for impulsive orientation of linear and even asymmetric top molecules under field-free condition (see, e.g. (7), and references therein).

Owing to the symmetry of light interaction with the induced dipole moment, strong laser fields with fixed linear polarization can be utilized only to align, but not orient, molecules in space. In contrast, fields with twisting polarization break this symmetry, and were predicted to transiently orient chiral molecules (8–10), as was recently confirmed experimentally (11).

Here we report a related, yet fundamentally new phenomenon – field-free *persistent* enantioselective orientation (PESO) of chiral molecules, which lasts orders of magnitude longer than the duration of the exciting laser pulses. This effect is unique for chiral molecules driven

by nonresonant laser fields with twisted polarization. In all the previously known approaches to impulsive molecular orientation, including techniques using single-cycle THz pulses (12–18), alone or in combination with optical pulses (19–21), or two-color laser fields (7, 13, 22–28), the post-pulse orientation shows transient signals with zero time average. To the best of our knowledge, our paper presents the first demonstration of the long-lasting permanent molecular orientation induced by a pulsed optical field.

Long-lived orientation of chiral molecules induced by laser fields with twisted polarization was recently theoretically predicted in (9, 10, 29). Several possible examples of such fields include a pair of delayed cross-polarized laser pulses (30, 31), chiral pulse trains (32–34), polarization-shaped pulses (35–37) and an optical centrifuge (38–42).

In what follows, we present the first experimental observation of the PESO phenomenon, using chiral propylene oxide molecules spun by an optical centrifuge. The results of experimental measurements are in a good agreement with the theoretical predictions.

## Experimental Methods and Results

Our setup for producing the field of an optical centrifuge has been built according to the original recipe of Karzmarek et al. (38) and has been described in an earlier publication (43). Briefly, we split the spectrum of broadband laser pulses from a Ti:sapphire amplifier (10 mJ, 35 fs, repetition rate 1 KHz, central wavelength 795 nm) in two equal parts using a Fourier pulse shaper. The two beams are first frequency chirped with a chirp rate  $\beta$  of equal magnitude and opposite sign ( $\beta = \pm 0.3$

<sup>a)</sup> Electronic mail: [ilya.averbukh@weizmann.ac.il](mailto:ilya.averbukh@weizmann.ac.il)

<sup>b)</sup> Electronic mail: [vmilner@phas.ubc.ca](mailto:vmilner@phas.ubc.ca)

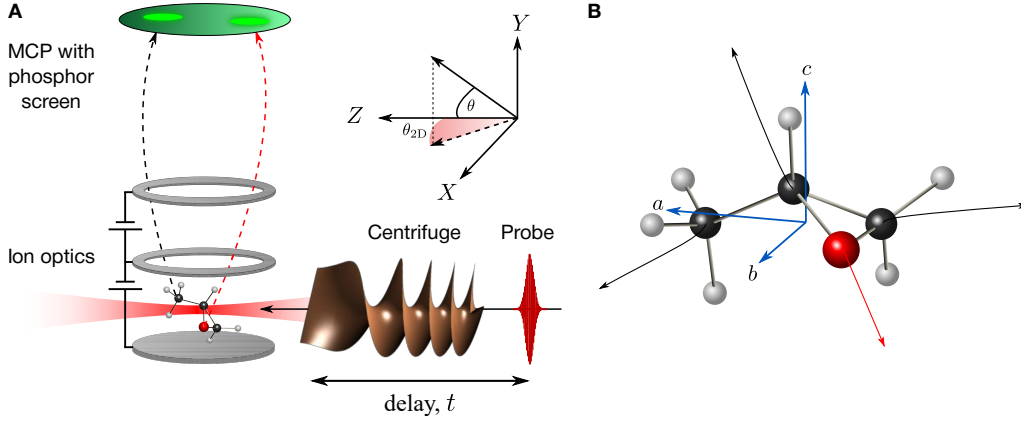


**Fig. 1.** (A) Schematic illustration of our experimental geometry. Cold PPO molecules in a seeded helium jet are spun in an optical centrifuge and Coulomb exploded with a probe pulse between the plates of a conventional velocity map imaging spectrometer, equipped with a multi-channel plate (MCP) detector and a phosphor screen. The inset shows the fixed frame axes and the definition of angles  $\theta$  and  $\theta_{2D}$  used in text. (B) Right-handed enantiomer of propylene oxide, (*R*)-PPO, depicted in the frame of its principal axes  $a$ ,  $b$ , and  $c$  (the corresponding moments of inertia satisfy  $I_a < I_b < I_c$ );  $a$  axis is close to the principal axis of polarizability tensor with highest polarization value. Red, black, and gray spheres represent oxygen, carbon, and hydrogen atoms, respectively. Coulomb explosion trajectories from a stationary molecule are shown with thin black and red lines (see Theoretical Methods section for details).

THz/ps). The chirped beams are then circularly polarized with an opposite sense of circular polarization. Optical interference of these laser fields results in a pulse illustrated in Fig. 1A: its polarization vector is rotating in  $XY$  plane with an instantaneous angular frequency  $\Omega = 2\beta t$ . The duration of our centrifuge pulse is 20 ps.

We use a typical velocity map imaging (VMI) setup in which the molecular jet is intercepted by intense femtosecond probe beam between the plates of a time-of-flight spectrometer (see Fig. 1A). Multiple ionization of a molecule by the probe beam results in Coulomb explosion, i.e. breaking of the molecule into ionized fragments. As the fragment ions accelerate towards, and impinge on, the multi-channel plate detector (MCP), the projection of their velocities on the  $XZ$  plane is mapped on the plane of the detector. Mass selectivity is provided by gating the MCP at the time of arrival of the fragment of interest. A simplified model of Coulomb explosion shown in Fig. 1B predicts that the velocities of  $C^+$  ions (averaged over three carbon atoms) and  $O^+$  ions have opposite projections on the laboratory  $Z$  axis (see Fig. 3), in full agreement with the experimental observations (see Fig. 2).

We extract the information about the molecular orientation in the laboratory frame as a function of time by recording VMI images at different centrifuge-probe time delays (see Fig. 1A). The experimental observable, bearing the information about the degree of orientation, is conventionally determined as  $\langle \cos(\theta_{2D}) \rangle$ . Here  $\theta_{2D}$  is the angle between the projection of the fragment's velocity  $\mathbf{v}$  on the velocity map imaging detector plane ( $XZ$  plane) and the laboratory  $Z$  axis,  $\langle \dots \rangle$  implies averaging over the molecular ensemble. Positive (negative) values of  $\langle \cos(\theta_{2D}) \rangle$  reflect the orientation of  $\mathbf{v}$  along (against)

the laboratory  $Z$  axis. In practice, an average of a few million ion fragments were recorded for each set of experimental conditions, resulting in the precision of  $10^{-3}$  in determining  $\langle \cos(\theta_{2D}) \rangle$ . To minimize systematic errors, e.g. due to the inhomogeneous response of our detector as well as long-term drifts in molecular density and laser intensity, we define the following quantity (hereafter referred to as the “2D orientation factor”):

$$\Delta \langle \cos(\theta_{2D}) \rangle \equiv \langle \cos(\theta_{2D}) \rangle_{\odot} - \langle \cos(\theta_{2D}) \rangle_{\ominus},$$

where the indices  $\odot$  and  $\ominus$  correspond to the clockwise and counter-clockwise direction of polarization rotation, as observed along the laser beam propagation. In Fig. 2 we plot the experimentally measured  $\Delta \langle \cos(\theta_{2D}) \rangle$  for the velocity distributions of  $O^+$  and  $C^+$  fragments. For both, the enantioselective effect of the centrifuge is reflected by the opposite sign of the 2D orientation factor for the two enantiomers. In the case of oxygen ions (Fig. 2A),  $|\Delta \langle \cos(\theta_{2D}) \rangle|$  reaches the values of the order of  $10^{-2}$  during the interaction with the centrifuge field (first 20 ps), being positive for left- and negative for right-handed molecules. When the interaction is over, the degree of orientation become smaller, but maintain a non-zero value of opposite signs for at least 700 ps (a maximum accessible delay time in the current experimental setup). Carbon ions demonstrate similar behavior, shown in Fig. 2B. The non-zero 2D orientation factor of  $C^+$  also persists on the full available time scale. As seen, the orientation signals of  $O^+$  and  $C^+$  ions are opposite to each other for both enantiomers, in agreement with theoretical simulations (see Fig. 3).

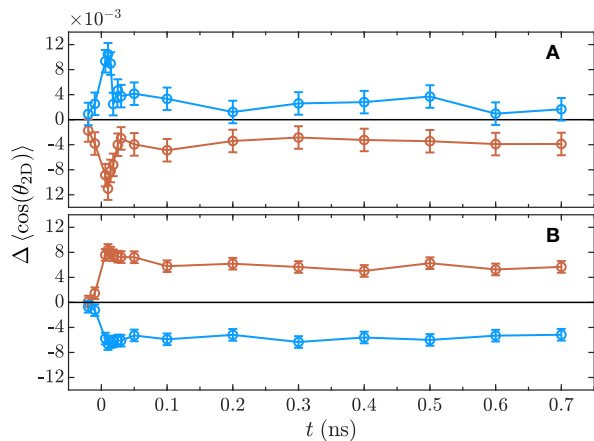


**Fig. 2.** Experimentally measured 2D orientation factor in the velocity distribution of (A)  $O^+$  and (B)  $C^+$  fragments as a function of optical centrifuge-probe pulse delay,  $t$ . Orange - right handed molecule, (*R*)-PPO; blue - left handed molecule, (*S*)-PPO. Note the reversal of colors between the two plots.

### Theoretical Methods and Results

The chiral molecule is modeled as rigid asymmetric top having anisotropic polarizability. We carry out both classical and fully quantum simulations of the laser driven rotational dynamics. For the classical simulations, the behavior of a thermal ensemble was treated using the Monte Carlo approach. Our numerical scheme relies on solving the coupled system of Euler equations and quaternions equations of motion (44). The molecular parameters and details of the scheme may be found in (10).

For the quantum simulations, we use the symmetric-top wavefunctions  $|JKM\rangle$  as a basis set. Here  $J$  is the total angular momentum,  $K$  is its projection on the molecule-fixed  $a$  axis, and  $M$  is its projection onto the laboratory fixed  $Z$  axis (45). The interaction potential is expressed in terms of Wigner D-matrices. Using a unitary transformation, the matrices are transformed to the asymmetric-top basis. Details of the scheme may be found in (29).

We adopted a simplified model of Coulomb explosion, which assumes an instantaneous conversion of all constituent atoms into singly charged ions, while keeping the molecular configuration unchanged during the interaction with the probe pulse. For finding the asymptotic velocities of all ions after the Coulomb explosion, we numerically solved the system of coupled Newton's equations. As the kinetic energy of the fragments due to Coulomb explosion exceeds the rotational energy, we neglected the rotational velocities of the atoms at the moment of explosion. Trajectories of the fragments are shown in Fig. 1B by red and black arrowed lines for oxygen and carbon ions, respectively. A static PPO molecule would eject its ions along these directions that carry the information about the spatial orientation of

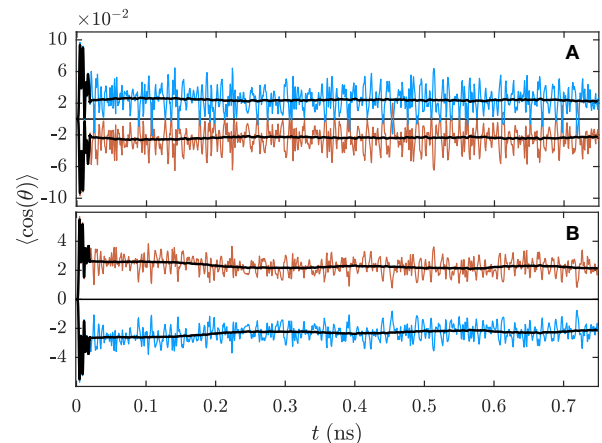


**Fig. 3.** (A) 3D orientation factor of the oxygen ion velocity. (B) 3D orientation factor of the carbon ion velocity (averaged over the three carbons). Orange - (*R*)-PPO; light blue - (*S*)-PPO. Solid black curves are a 100 ps time-averages,  $\overline{\langle \cos(\theta) \rangle}(t) = \frac{1}{\Delta t} \int_{t-\Delta t/2}^{t+\Delta t/2} \langle \cos(\theta) \rangle(t') dt'$  of the signals. Parameters of the optical centrifuge pulse are: peak intensity  $I_0 = 5 \times 10^{12} \text{ W/cm}^2$ ,  $\beta = 0.05 \text{ ps}^{-2}$ , duration  $t_p = 20 \text{ ps}$ . Initial rotation temperature was set to  $T = 0 \text{ K}$ .

the molecule at the moment of explosion.

Figure 3 shows the results of our simulations, and presents the conventional (3D) orientation factors,  $\langle \cos(\theta) \rangle$  - the expectation values of the projection of oxygen and carbon ions velocity vectors on the laser propagation direction ( $Z$  axis in Fig. 1A). Here  $\theta$  is the angle between the velocity vector and the  $Z$  axis, and  $\langle \dots \rangle$  denotes ensemble average or quantum expectation value for the classical and quantum mechanical simulations, respectively. The presented orientation factor for the carbon ions was obtained by averaging the results for the three individual molecular carbons. Similar to the experimental results, the orientation factors of both oxygen and carbon ions are non-zero long after the end of the optical centrifuge pulse. Note, that these factors have opposite signs for oxygen and carbon. A detailed analysis shows the reason for this. When the molecular  $a$  axis was trapped by the optical centrifuge and rotated in the  $XY$  plane, the molecule turned about the  $a$  axis such that the middle carbon and oxygen atoms happened to be on the opposite sides of the  $XY$  plane. As the result of the Coulomb explosion, the two end carbon ions recoil close to the plane, while the middle carbon and the oxygen ions fly apart on different sides of the  $XY$  plane, resulting in the opposite orientation factors. The observed permanent orientation is enantioselective and opposite for the two enantiomers.

It is interesting to consider the dynamics of molecules during their interaction with the optical centrifuge, which eventually leads to the field-free PESO phenomenon. Figure 4A,B shows the distribution of the angular momentum magnitude (in units of  $\hbar$ ) as a function of time during the optical centrifuge operation (20 ps).

It is evident that the molecules undergo a forced angular acceleration. Figure 4C shows the simulated (both classically and quantum mechanically) 3D orientation factors during the first 20 ps of the evolution. Solid black curve represents the envelope of the optical centrifuge field showing that the peak intensity is reached after 2 ps. During this initial stage, molecules are aligned in the direction of the (barely) rotating polarization, while their orientation remains zero. The latter rises only after the polarization twist becomes substantial and induces an orienting torque in the direction of the aligned most polarizable molecular axis  $a$  (see Fig. 1B). This supports the orientation mechanism described in (9, 10). The 3D orientation factors reach their persistent values of  $\langle \cos(\theta) \rangle \approx 2.5 \times 10^{-2}$  and  $\langle \cos(\theta) \rangle \approx 2.3 \times 10^{-2}$  for oxygen and carbon, respectively, after approximately 12 ps. Further acceleration is of little effect on the level of orientation. For computational reasons, the angular ac-

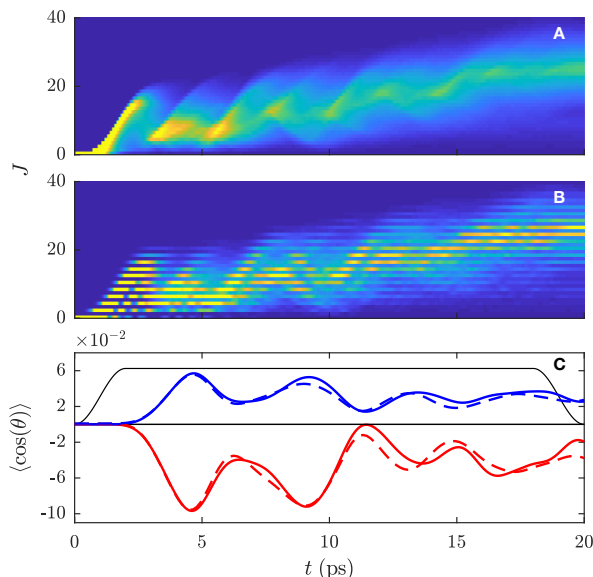


**Fig. 4.** (A,B) Distribution of the angular momentum in units of  $\hbar$ ,  $J$  as a function of time calculated (A) classically and (B) quantum mechanically. (C) Short time dynamics of the 3D orientation factors (for  $(R)$ -PPO). Solid blue and red curves are results of quantum mechanical simulation for carbon and oxygen ions velocities, respectively, whereas dashed lines show the results of classical simulations. Solid black line represents the intensity profile of the optical centrifuge field in arbitrary units. Parameters of the optical centrifuge are the same as in Fig. 3.

celeration used in our simulation is lower than the experimental one (by a factor of 6). The maximum attainable magnitude of the angular momentum,  $J_{\max}$  is proportional to the product  $t_p \beta$ , while the basis size required for full quantum simulations of asymmetric-top molecule scales as  $J_{\max}^3$ . The cubic scaling forbids the direct quantum calculation involving very high angular momentum states, although some progress is offered by the semi-classical methods (46). Moreover, at high  $J$  values, the

rigid-top approximation becomes invalid. However, even with the chosen  $\beta$  value, our simulations qualitatively reproduce the observed effect. Figure 4 suggests that the degree of molecular orientation does not necessarily benefit from the acceleration to progressively higher angular velocities, as only the initial stage of the accelerated spinning contributes to the desired orientation effect.

## Conclusions

We demonstrated both theoretically and experimentally the persistent enantioselective orientation (PESO) of chiral molecules induced by laser fields with twisted polarization. Theoretically, we found very good agreement between the classical and quantum approaches in the experimentally relevant range of parameters. The molecular orientation direction depends on both the sense of polarization twisting and the handedness of the molecule.

This long-lasting orientation provides new modalities for controlling the motion of chiral molecules, detecting molecular chirality by means of nonlinear optics, and potentially for separating the laser-oriented enantiomers in external inhomogeneous fields (see e.g. (47–49), references therein, and recent reviews (3, 4, 50)).

## References and Notes

- 1 F. A. Cotton. *Chemical Applications of Group Theory*. John Wiley & Sons, Hoboken, NJ, USA, 3<sup>rd</sup> edition, 1990.
- 2 C. P. Koch, M. Lemesko, and D. Sugny. Quantum control of molecular rotation. *arXiv: 1810.11338v1 [quant-ph]*, *Rev. Mod. Phys.* in press, 2019.
- 3 M. Lemesko, R. V. Krems, J. M. Doyle, and S. Kais. Manipulation of molecules with electromagnetic fields. *Mol. Phys.*, 111(12-13):1648–1682, 2013.
- 4 S. Fleischer, Y. Khodorkovsky, E. Gershnel, Y. Prior, and I. Sh. Averbukh. Molecular alignment induced by ultrashort laser pulses and its impact on molecular motion. *Isr. J. Chem.*, 52(5):414–437, 2012.
- 5 Y. Ohshima and H. Hasegawa. Coherent rotational excitation by intense nonresonant laser fields. *Int. Rev. Phys. Chem.*, 29(4):619–663, 2010.
- 6 H. Stapelfeldt and T. Seideman. Colloquium: Aligning molecules with strong laser pulses. *Rev. Mod. Phys.*, 75:543–557, Apr 2003.
- 7 K. Lin, I. Tutunnikov, J. Qiang, J. Ma, Q. Song, Q. Ji, W. Zhang, H. Li, F. Sun, X. Gong, H. Li, P. Lu, H. Zeng, Y. Prior, I. Sh. Averbukh, and J. Wu. All-optical field-free three-dimensional orientation of asymmetric-top molecules. *Nat. Commun.*, 9(1):5134, 2018.
- 8 A. Yachmenev and S. N. Yurchenko. Detecting chirality in molecules by linearly polarized laser fields. *Phys. Rev. Lett.*, 117:033001, 2016.
- 9 E. Gershnel and I. Sh. Averbukh. Orienting asymmetric molecules by laser fields with twisted polarization. *Phys. Rev. Lett.*, 120:083204, 2018.
- 10 I. Tutunnikov, E. Gershnel, S. Gold, and I. Sh. Averbukh. Selective orientation of chiral molecules by laser fields with twisted polarization. *J. Phys. Chem. Lett.*, 9(5):1105–1111, 2018.
- 11 A. A. Milner, J. A. M. Fordyce, I. MacPhail-Bartley, W. Wasserman, V. Milner, I. Tutunnikov, and I. Sh. Averbukh. Controlled

- enantioselective orientation of chiral molecules with an optical centrifuge. *Phys. Rev. Lett.*, 122:223201, 2019.
- <sup>12</sup>H. Harde, S. Keiding, and D. Grischowsky. THz commensurate echoes: Periodic rephasing of molecular transitions in free-induction decay. *Phys. Rev. Lett.*, 66:1834–1837, 1991.
  - <sup>13</sup>C. M. Dion, A. D. Bandrauk, O. Atabek, A. Keller, H. Umeda, and Y. Fujimura. Two-frequency IR laser orientation of polar molecules. Numerical simulations for HCN. *Chem. Phys. Lett.*, 302(3-4):215–223, 1999.
  - <sup>14</sup>I. Sh. Averbukh and R. Arvieu. Angular focusing, squeezing, and rainbow formation in a strongly driven quantum rotor. *Phys. Rev. Lett.*, 87:163601, 2001.
  - <sup>15</sup>M. Machholm and N. E. Henriksen. Field-free orientation of molecules. *Phys. Rev. Lett.*, 87:193001, 2001.
  - <sup>16</sup>S. Fleischer, Y. Zhou, R. W. Field, and K. A. Nelson. Molecular orientation and alignment by intense single-cycle THz pulses. *Phys. Rev. Lett.*, 107:163603, 2011.
  - <sup>17</sup>K. Kitano, N. Ishii, N. Kanda, Y. Matsumoto, T. Kanai, M. Kuwata-Gonokami, and J. Itatani. Orientation of jet-cooled polar molecules with an intense single-cycle THz pulse. *Phys. Rev. A*, 88:061405, 2013.
  - <sup>18</sup>R. Damari, S. Kallush, and S. Fleischer. Rotational control of asymmetric molecules: Dipole- versus polarizability-driven rotational dynamics. *Phys. Rev. Lett.*, 117:103001, 2016.
  - <sup>19</sup>D. Daems, S. Guérin, D. Sugny, and H. R. Jauslin. Efficient and long-lived field-free orientation of molecules by a single hybrid short pulse. *Phys. Rev. Lett.*, 94:153003, 2005.
  - <sup>20</sup>E. Gershnabel, I. Sh. Averbukh, and R. J. Gordon. Orientation of molecules via laser-induced antialignment. *Phys. Rev. A*, 73:061401, 2006.
  - <sup>21</sup>K. N. Egodapitiya, S. Li, and R. R. Jones. Terahertz-induced field-free orientation of rotationally excited molecules. *Phys. Rev. Lett.*, 112:103002, 2014.
  - <sup>22</sup>M. J. J. Vrakking and S. Stolte. Coherent control of molecular orientation. *Chem. Phys. Lett.*, 271(4-6):209–215, 1997.
  - <sup>23</sup>T. Kanai and H. Sakai. Numerical simulations of molecular orientation using strong, nonresonant, two-color laser fields. *J. Chem. Phys.*, 115(12):5492–5497, 2001.
  - <sup>24</sup>S. De, I. Znakovskaya, D. Ray, F. Anis, Nora G. Johnson, I. A. Bocharova, M. Magrakvelidze, B. D. Esry, C. L. Cocke, I. V. Litvinyuk, and M. F. Kling. Field-free orientation of CO molecules by femtosecond two-color laser fields. *Phys. Rev. Lett.*, 103:153002, 2009.
  - <sup>25</sup>K. Oda, M. Hita, S. Minemoto, and H. Sakai. All-optical molecular orientation. *Phys. Rev. Lett.*, 104:213901, 2010.
  - <sup>26</sup>J. Wu and H. Zeng. Field-free molecular orientation control by two ultrashort dual-color laser pulses. *Phys. Rev. A*, 81:053401, 2010.
  - <sup>27</sup>E. Frumker, C. T. Hebeisen, N. Kajumba, J. B. Bertrand, H. J. Wörner, M. Spanner, D. M. Villeneuve, A. Naumov, and P. B. Corkum. Oriented rotational wave-packet dynamics studies via high harmonic generation. *Phys. Rev. Lett.*, 109:113901, 2012.
  - <sup>28</sup>N. Takemoto and K. Yamanouchi. Fixing chiral molecules in space by intense two-color phase-locked laser fields. *Chem. Phys. Lett.*, 451(1):1 – 7, 2008.
  - <sup>29</sup>I. Tutunnikov, J. Floß, E. Gershnabel, P. Brumer, and I. Sh. Averbukh. Laser induced persistent orientation of chiral molecules. *arXiv: 1905.12609 [physics.chem-ph]*, 2019.
  - <sup>30</sup>S. Fleischer, Y. Khodorkovsky, Y. Prior, and I. Sh. Averbukh. Controlling the sense of molecular rotation. *New J. Phys.*, 11(10):105039, 2009.
  - <sup>31</sup>K. Kitano, H. Hasegawa, and Y. Ohshima. Ultrafast angular momentum orientation by linearly polarized laser fields. *Phys. Rev. Lett.*, 103:223002, 2009.
  - <sup>32</sup>S. Zhdanovich, A. A. Milner, C. Bloomquist, J. Floß, I. Sh. Averbukh, J. W. Hepburn, and V. Milner. Control of molecular rotation with a chiral train of ultrashort pulses. *Phys. Rev. Lett.*, 107:243004, 2011.
  - <sup>33</sup>C. Bloomquist, S. Zhdanovich, A. A. Milner, and V. Milner. Directional spinning of molecules with sequences of femtosecond pulses. *Phys. Rev. A*, 86:063413, 2012.
  - <sup>34</sup>J. Floß and I. Sh. Averbukh. Molecular spinning by a chiral train of short laser pulses. *Phys. Rev. A*, 86:063414, 2012.
  - <sup>35</sup>G. Karras, M. Ndong, E. Hertz, D. Sugny, F. Billard, B. Lavorel, and O. Faucher. Polarization shaping for unidirectional rotational motion of molecules. *Phys. Rev. Lett.*, 114:103001, Mar 2015.
  - <sup>36</sup>E. Prost, H. Zhang, E. Hertz, F. Billard, B. Lavorel, P. Bejot, J. Zyss, I. Sh. Averbukh, and O. Faucher. Third-order-harmonic generation in coherently spinning molecules. *Phys. Rev. A*, 96:043418, 2017.
  - <sup>37</sup>E. Prost, E. Hertz, F. Billard, B. Lavorel, and O. Faucher. Polarization-based tachometer for measuring spinning rotors. *Opt. Express*, 26(24):31839–31849, 2018.
  - <sup>38</sup>J. Karczmarek, J. Wright, P. Corkum, and M. Ivanov. Optical centrifuge for molecules. *Phys. Rev. Lett.*, 82:3420–3423, 1999.
  - <sup>39</sup>D. M. Villeneuve, S. A. Aseyev, P. Dietrich, M. Spanner, M. Yu. Ivanov, and P. B. Corkum. Forced molecular rotation in an optical centrifuge. *Phys. Rev. Lett.*, 85:542–545, 2000.
  - <sup>40</sup>L. Yuan, S. W. Teitelbaum, A. Robinson, and A. S. Mullin. Dynamics of molecules in extreme rotational states. *Proc. Natl. Acad. Sci. U. S. A.*, 108(17):6872–6877, 2011.
  - <sup>41</sup>A. Korobenko, A. A. Milner, and V. Milner. Direct observation, study, and control of molecular superrotors. *Phys. Rev. Lett.*, 112:113004, 2014.
  - <sup>42</sup>A. Korobenko. Control of molecular rotation with an optical centrifuge. *J. Phys. B*, 51(20):203001, 2018.
  - <sup>43</sup>A. Korobenko, A. A. Milner, J. W. Hepburn, and V. Milner. Rotational spectroscopy with an optical centrifuge. *Phys. Chem. Chem. Phys.*, 16:4071–4076, 2014.
  - <sup>44</sup>D. C. Rapaport. *The Art of Molecular Dynamics Simulation*. Cambridge University Press, 2<sup>nd</sup> edition, 2004.
  - <sup>45</sup>R. Zare. *Angular momentum : understanding spatial aspects in chemistry and physics*. Wiley, New York, 1988.
  - <sup>46</sup>H. Schmiedt, S. Schlemmer, S. N. Yurchenko, A. Yachmenev, and P. Jensen. A semi-classical approach to the calculation of highly excited rotational energies for asymmetric-top molecules. *Phys. Chem. Chem. Phys.*, 19:1847–1856, 2017.
  - <sup>47</sup>E. Gershnabel and I. Sh. Averbukh. Electric deflection of rotating molecules. *J. Chem. Phys.*, 134(5):054304, 2011.
  - <sup>48</sup>E. Gershnabel and I. Sh. Averbukh. Deflection of rotating symmetric top molecules by inhomogeneous fields. *J. Chem. Phys.*, 135(8):084307, 2011.
  - <sup>49</sup>A. Yachmenev, J. Onvlee, E. Zak, A. Owens, and J. Küpper. Field-induced diastereomers for chiral separation. *arXiv: 1905.07166 [physics.chem-ph]*, 2019.
  - <sup>50</sup>Y.-P. Chang, D. A. Horke, S. Trippel, and J. Küpper. Spatially-controlled complex molecules and their applications. *Int. Rev. Phys. Chem.*, 34(4):557–590, 2015.

**Acknowledgments:** This work was supported by the Israel Science Foundation (Grant No. 746/15), the ISF-NSFC joint research program (Grant No. 2520/17), and by Natural Sciences and Engineering Research Council of Canada grants to P.B. and V.M. The work of A.A.M. and V.M. was carried out under the auspices of the Canadian Center for Chirality Research on Origins and Separation (CHIROS), funded by Canada Foundation for Innovation. I.A. acknowledges support as the Patricia Elman Bildner Professorial Chair, and thanks the UBC Department of Physics & Astronomy for hospitality extended to him during his sabbatical stay. This research was made possible in part by the historic generosity of the Harold Perlman Family. **Author contributions:** I.T., I.A., P.B., and V.M. initiated the study. A.A.M. and V.M. designed and carried out the experiment. I.T., J.F.,

E.G. performed the simulations. I.A., P.B., and V.M. supervised and guided the work. All authors contributed to the data analysis and writing the

manuscript. **Competing interests:** The authors declare that they have no competing interests.